Published in IET Communications
Received on 6th April 2011
Revised on 2nd October 2011
doi: 10.1049/iet-com.2011.0269

ISSN 1751-8628

Cyclostationarity-based soft cooperative spectrum sensing for cognitive radio networks

H. Sadeghi P. Azmi H. Arezumand

Department of Electrical and Computer Engineering, Tarbiat Modares University, Tehran, Iran
E-mail: pazmi@modares.ac.ir

Abstract: Reliable detection of primary users (PUs) in the presence of interference and noise is a crucial problem in cognitive radio networks. To address the above issue, cooperative spectrum sensing based on cyclostationary feature detection that can robustly detect weak primary signals has been proposed in the literature. Among different cooperative techniques, in this study the authors focus on combination of soft decisions derived based on asymptotic properties of cyclic autocorrelation estimates. The objective is to maximise deflection coefficient performance metric at the fusion centre, where linear combination of cyclostationary soft decisions is performed. Since the proposed method allows for distributed cyclostationarity spectrum sensing, it is more reliable and faster than non-cooperative traditional multi-cycle cyclostationarity detection schemes. To reduce the computational complexity of the exact distribution of proposed test statistic at fusion centre, the authors derive efficient approximations for the distribution under null and alternative hypotheses. Extensive simulation results in different scenarios demonstrate the advantage of the proposed method and confirm the analytic performance characterisations. In addition, the authors study the impact of mobility of cognitive devices on the cyclostationarity of received signals and verify our analysis via simulation.

1 Introduction

Cognitive radio (CR), first introduced by Mitola in 1999 [1], provides a way to use the valuable radio spectrum in an efficient manner. These radios are actually unlicensed wireless devices that temporarily utilise the unused primary spectral bands [2–5]. However, the first step in opportunistic access to the licensed spectrum is the detection of unused spectral bands [6–8]. In addition, CR should vacate the primary band as soon as a primary user (PU) starts transmitting. Briefly speaking, the transmission opportunity exploitation and PU detection are main challenges to CR networks.

To reliably detect the existence of PUs, CRs must be able to detect very weak signals, or in other words, work in very low signal-to-noise ratio (SNR) environments [9]. Detection of cyclostationary (CS) features, which are inherent properties of digital modulated signals, has been proposed in the literature to overcome this problem [10–12]. In fact, it is well known that if a signal has strong CS properties, it can be detected at very low SNRs [6]. In addition, CS detectors can inherently distinguish PUs from secondary users as well as interferers, if they have dissimilar cyclic features. Conventional energy detectors cannot satisfy this important requirement [6]. Although CS detectors operate much better than energy ones, but they are generally more complex [13].

To achieve further improvement in sensing performance even in the face of fading and shadowing, cooperative spectrum sensing (CSS) in secondary networks has been proposed as a promising scheme. In fact, cooperative sensing among spatially distributed SUs can mitigate effects of shadowing and fading [11] and leads to more reliable detectors. However, most of researches carried out in literature is based on the energy detection method at each node of secondary network. Recently, cyclostationarity-based CSS has been proposed in the literature, for example in [11, 14]. In this paper, we consider cooperative fusion in a secondary network within which each CR performs its spectrum sensing via cyclostationarity-based detection scheme. The primary objective of this policy is 2-fold: (i) to assure reliable performance at low SNRs, because of exploiting the powerful CS-based sensing at each node; and (ii) to overcome the fading impairments and reduce the sensing time required at each node of the network.

Among existing single-user CS feature detection methods, we employ the well-known Dandawaté–Giannakis's [15] algorithm, recently modified in [11]. The main idea of this method is to consistently estimate the cyclic autocorrelation function (CAF), which approaches zero except at cycle frequencies of the CS signal. Based on the asymptotic complex normality of CAF estimation error, a statistical test for the presence of a cycle frequency of interest has been proposed in [15]. Although the hypothesis testing scheme proposed in [15] is computationally extensive, but it has good performance and can be applied when some transmission parameters of the PU are known to the CR receiver. This assumption is almost true in cases that CRs are to work in IEEE 802.22 wireless regional area networks (WRANs). The CS feature we consider here is the symbol period of PU signal. Even if the symbol rate is unknown, it can be estimated simply and accurately [16, 17].

Cyclostationarity-based hard [14] and soft [11] CSS strategies have been proposed for global inference at fusion centre (FC) of the secondary network. However proposed methods are not optimal. In fact, the system-wide optimal solution is obtained by performing likelihood ratio tests in both FC and SUs [18]. However, minimising the overall average cost of the network and obtaining the resultant global and local optimal thresholds is not a straightforward problem, since the local secondary users are coupled with each other. Therefore finding the local optimal thresholds in hard-decision-based cooperative sensing is difficult [18]. In this paper, instead of finding the optimal thresholds, we propose that each secondary user independently performs local CS sensing and then sends its decision statistic to the FC. Consequently, only the optimal test should be performed at the FC.

In soft decision-based context, the authors in [11] proposed summing different cyclostationarity-based test statistics transmitted by CRs. In this paper, we improve the cooperative sum detector of [11] to yield a higher probability of detection. As we will show later, sensing performance can be improved by properly scaling the transmitted test statistics. To this end, we will find the weights so as to maximise two optimality criteria: the conventional deflection coefficient (CDC) as well as the modified deflection coefficient (MDC) [19]. For the sake of comparison, we will also propose a scaled version of sum detector, whose performance is the same as the sum detector of [11]. In addition, we will discuss the performance of the proposed schemes through analysis as well as simulation experiments. Since there is not a simple and accurate closed-form expression for the distribution of resultant test statistic at the fusion rule, we will also propose an efficient approximate distribution. Furthermore, we will show that the proposed approximation method has enough accuracy, in terms of calculating the probability density function of the proposed test statistic under null and alternative hypotheses. This approximation method allows threshold setting at the FC.

Finally, we analytically characterise the impact of secondary user's mobility on its CS sensing capability. Under some conditions, we will show that the cyclostationarity of received signals vary proportional to the autocorrelation of channel fading process. Furthermore, the impact of fading depends on the signalling structure of PUs.

The remainder of this paper is organised as follows. Section 2 briefly reviews the system model and definitions related to prior works. Section 3 summarises the signal detection algorithm employed in local secondary users and its associated test statistic. Section 4 establishes the proposed CSS procedures. Section 5 describes the proposed approximate distribution for the hypothesis testing rule at FC, and its analytical performance evaluation. Section 6 presents the simulations results. Finally, we draw the conclusions in Section 7. In addition, the impact of secondary user's mobility on local cyclostationarity sensing is analytically characterised in Appendix 2.

2 System model

Since mobile communication is one of the most likely applications of CR, we must consider the cyclostationarity detection problems in Rayleigh fading channels [10]. In this paper we assume Rayleigh flat fading channel between CRs and PU. The based-band discrete-time received signal for ith CR, $y_i(n)$, $i = 1, 2, \ldots, L$, at time instance n is

$$y_i(n) = \eta h_i(n)x(n) + w_i(n), \quad n = 1, \ldots, M \tag{1}$$

where $h_i(n)$ and $w_i(n)$ are complex channel fading and stationary complex white Gaussian noise processes, respectively, which are circularly symmetric complex-valued Gaussian random variables. In other words, $h_i(n) \sim \mathcal{CN}(0, \sigma_i^2)$ and $w_i(n) \sim \mathcal{CN}(0, N_i)$, where σ_i^2 and N_i are variances of fading and additive Gaussian noise distributions. Moreover, $\eta = 0$ and 1 correspond to null (inactive PU) and alternative (active PU) hypotheses, respectively. In this paper, we assume that during the length-M time interval the PU is either active or inactive. The signal transmitted by PU is denoted by $x(n)$. Without loss of generality, $x(n)$, $\{h_i(n)\}$ and $\{w_i(n)\}$ are assumed to be independent of each other. Also we note that the secondary FC can be a base station or a secondary user with higher computational capabilities. It is assumed that L secondary users exist in network. Throughout this paper, the reporting channels are assumed to be noise free.

The detection problem we are encountering at each SU is testing for the presence of cyclostationarity in the received signal. In the sequel, we mean by cyclostationarity the discrete-time second-order CS property in the wide sense. In this context, a signal $x(n)$ is said to show cyclostationarity at a cycle frequency of interest α, if the CAF is not identically zero [15].

In this paper, conditional independence of spatially distributed SUs is assumed [11], so the test statistics computed at local sensors are asymptotically conditionally independent given either hypothesis. Furthermore, it is assumed that each SU performs CS detection at a single or different cycle frequencies. This causes the network to perform parallel and reliable spectrum sensing in a short period of time, and improves the agility of secondary network. In addition, this allows for distributed single- or multi-cycle detection.

3 Local cyclostationarity sensing

The CS detector we propose for each node of secondary network is based on the generalised likelihood ratio test derived in [15]. This statistical test detects the presence of cycles appeared in the second-order cyclic cumulants and does not assume any specific distribution on the transmitted data [15]. In this section we overview the key results of [11, 15], required for developing the new cooperative test statistic.

Assume that we want to test for cyclostationarity in signal $x(n)$. The discrete-time unbiased and consistent estimation of the CAF of $x(n)$ is given by [15]

$$\hat{R}^{\alpha}_{xx^*}(\tau) \triangleq \frac{1}{M}\sum_{n=1}^{M} x(n)x^*(n+\tau)\mathrm{e}^{-\mathrm{j}2\pi\alpha n} \tag{2}$$

where τ and α refer to the discrete time lag and cycle frequency, respectively. We define a vector consisting of CAF estimates of multiple time lags $\{\tau_i\}_{i=1}^{N}$ for a candidate cycle frequency α as

$$\hat{\boldsymbol{r}}_{xx^*} \triangleq [\mathrm{Re}\{\hat{R}^{\alpha}_{xx^*}(\tau_1)\}, \ldots, \mathrm{Re}\{\hat{R}^{\alpha}_{xx^*}(\tau_N)\}, \mathrm{Im}\{\hat{R}^{\alpha}_{xx^*}(\tau_1)\}, \ldots, \mathrm{Im}\{\hat{R}^{\alpha}_{xx^*}(\tau_N)\}] \tag{3}$$

doi: 10.1049/iet-com.2011.0269

It has been proven that subject to certain mixing conditions, $\sqrt{M}\hat{\boldsymbol{r}}_{xx^*}$ is asymptotically (i.e. as $M \to \infty$) distributed as $\sqrt{M}\hat{\boldsymbol{r}}_{xx^*} \overset{\mathrm{D}}{\sim} \mathcal{N}(\boldsymbol{\mu}, \boldsymbol{\Sigma}_{xx^*})$, where $\boldsymbol{\mu} = \mathbf{0}$ under $\mathcal{H}_0$, and $\boldsymbol{\mu} = \sqrt{M}\boldsymbol{r}_{xx^*}$ under $\mathcal{H}_1$ [11]. Here, $\overset{\mathrm{D}}{\sim}$ denotes the convergence in distribution, and $\mathcal{N}(\boldsymbol{\mu}, \boldsymbol{V})$ denotes the multivariate normal distribution with mean vector $\boldsymbol{\mu}$ and covariance matrix $\boldsymbol{V}$.

Since $\boldsymbol{r}_{xx^*}$ is non-random [15], the distribution of $\hat{\boldsymbol{r}}_{xx^*}$ under $\mathcal{H}_0$ and $\mathcal{H}_1$ differs only in the mean. So, the asymptotic complex normality of $\hat{\boldsymbol{r}}_{xx^*}$ allows proposing the following generalised log-likelihood ratio (GLRT) [11, 15]:

$$\mathcal{T} = 2\ln\Lambda_{\mathrm{GLR}} = 2\ln\frac{f(\hat{\boldsymbol{r}}_{xx^*}|\mathcal{H}_1)}{f(\hat{\boldsymbol{r}}_{xx^*}|\mathcal{H}_0)} = M\hat{\boldsymbol{r}}_{xx^*}\hat{\boldsymbol{\Sigma}}_{xx^*}^{-1}\hat{\boldsymbol{r}}_{xx^*}^{\mathrm{T}} \tag{4}$$

where $\hat{\boldsymbol{\Sigma}}_{xx^*}$ is the estimated covariance matrix, which is described in Appendix 1. It has been proved in [11, 15] that the asymptotic distribution (i.e. $M \to \infty$) of $\mathcal{T}$ under both hypotheses is

$$\mathcal{T} \sim \begin{cases} \chi^2_{2N}, & \mathcal{H}_0 \\ \chi'^2_{2N}(\lambda), & \mathcal{H}_1 \end{cases} \tag{5}$$

where χ^2_r and $\chi'^2_r(\lambda)$ denote the central and non-central chi-squared random variable with r degrees of freedom, respectively. The non-centrality parameter of distribution under alternative hypothesis is given by $\lambda = M\boldsymbol{r}_{xx^*}\hat{\boldsymbol{\Sigma}}_{xx^*}^{-1}\boldsymbol{r}_{xx^*}^{\mathrm{T}}$, where the superscript $(\cdot)^{\mathrm{T}}$ represents the transpose operator [11].

Based on above discussions, we obtain the corresponding false-alarm and detection probabilities as

$$P_{\mathrm{f}} = \Pr\{\mathcal{T} > \gamma|\mathcal{H}_0\} = \frac{\Gamma(N, \gamma/2)}{\Gamma(N)} \tag{6}$$

$$P_{\mathrm{d}} = \Pr\{\mathcal{T} > \gamma|\mathcal{H}_1\} = \mathcal{Q}_{\mathrm{N}}(\sqrt{\lambda}, \sqrt{\gamma}) \tag{7}$$

where $\Gamma(a, x)$, $\Gamma(\cdot)$ and $\mathcal{Q}_N(a, b)$ denote the incomplete Gamma function, Gamma function and generalised Marcum Q function, respectively [20]. The local detection probability for a target probability of false alarm $\bar{P}_{\mathrm{f}}$ can be compactly represented as

$$P_{\mathrm{d}} = \mathcal{Q}_{\chi'^2_{2N}(\lambda)}(\mathcal{Q}^{-1}_{\chi^2_{2N}}(\bar{P}_{\mathrm{f}})) \tag{8}$$

where $\mathcal{Q}_{\chi'^2_{2N}(\lambda)}(x) \triangleq \int_x^\infty p(t)\,\mathrm{d}t$ is the right-tail probability for a $\chi'^2_r(\lambda)$ random variable with pdf $p(t)$. Since (8) is derived for asymptotic cases, we should evaluate it for different number of samples (i.e. M) and compare with Monte-Carlo simulation results. This issue is addressed in Section 6.

4 Proposed cooperative cyclostationarity-based sensing

In this section, we propose a cooperative sensing scheme where soft decisions from several SUs are combined linearly at the FC. The FC may be a separate secondary base station or one of the SUs. Assume that we want to simultaneously detect a candidate cycle frequency or a group of different cycles of interest from the set $\{\alpha_j\}_{j=1}^L$. Each SU is assigned a single (different or identical) cycle frequency. This causes the secondary network to effectively search for the presence of cycle frequencies in a parallel manner. Hence, reliable CS detection can be performed. Let $\mathcal{T}_j$ represents the CS test statistic for cycle frequency α_j computed at jth SU. Furthermore, we note that the test statistics $\mathcal{T}_j$ are asymptotically optimal in the generalised likelihood sense [15]. The proposed weighting scheme aims to maximise the deflection coefficient (DC) constructed from GLRTs received from different SUs. Intuitively, the more information secondary user j has, the more its contribution to making the final decision. We propose the following linear fusion rule for L test statistics transmitted by SUs

$$S(\boldsymbol{\Gamma}) \triangleq \mathcal{T}_{\mathrm{C}} = \sum_{j=1}^{L} w_j\mathcal{T}_j = \boldsymbol{w}^{\mathrm{T}}\boldsymbol{\Gamma} \underset{\mathcal{H}_0}{\overset{\mathcal{H}_1}{\gtrless}} \eta \tag{9}$$

In the above expression

$$\boldsymbol{w}^{\mathrm{T}} = [w_1, w_2, \ldots, w_L], \quad w_i \geq 0 \tag{10}$$

is the weight vector used to build the linear fusion rule, and

$$\boldsymbol{\Gamma}^{\mathrm{T}} = [\mathcal{T}_1, \mathcal{T}_2, \ldots, \mathcal{T}_L] \tag{11}$$

is the (observed) vector of test statistics.

The problem we are encountering is how we should calculate the weight vector (10), thereby the resultant detector (9) achieves the best performance. To this end, we choose the DC [21] as a performance metric. However, first- and second-order moments of $\mathcal{T}_{\mathrm{C}}$ are needed for derivation of the deflection of the cooperative detector. Since computing these moments under $\mathcal{H}_1$ requires the knowledge of non-centrality parameters at the SUs, we propose that each SU directly estimates the non-centrality parameter from the received signal at each sensing slot. To this end, each SU can approximately compute its non-centrality parameter under $\mathcal{H}_1$ from the received data as follows

$$\hat{\lambda} = M\hat{\boldsymbol{r}}_{xx^*}\hat{\boldsymbol{\Sigma}}_{xx^*}^{-1}\hat{\boldsymbol{r}}_{xx^*}^{\mathrm{T}} \tag{12}$$

Consequently, the value of estimated non-centrality parameter at each SU is equal to the computed test statistic over that sensing slot.

Based on above discussions, the mean and variance of the proposed test statistic (9) can be obtained for a dedicated sensing slot, as follows

$$\begin{aligned} E[\mathcal{T}_{\mathrm{C}}|\mathcal{H}_0] &= 2N\sum_{i=1}^{L} w_i \\ E[\mathcal{T}_{\mathrm{C}}|\mathcal{H}_1] &\simeq \sum_{i=1}^{L} w_i(2N + \hat{\lambda}_i) \\ \mathrm{Var}[\mathcal{T}_{\mathrm{C}}|\mathcal{H}_0] &= 4N\sum_{i=1}^{L} w_i^2 = 4N\boldsymbol{w}^{\mathrm{T}}\boldsymbol{w} \\ \mathrm{Var}[\mathcal{T}_{\mathrm{C}}|\mathcal{H}_1] &\simeq 4\sum_{i=1}^{L} w_i^2(N + \hat{\lambda}_i) = 4\boldsymbol{w}^{\mathrm{T}}\boldsymbol{\Psi}\boldsymbol{w} \end{aligned} \tag{13}$$

with

$$\boldsymbol{\Psi} \triangleq N\mathbf{I}_L + \mathbf{diag}(\boldsymbol{\Lambda}) \tag{14}$$

Here, **diag**(·) denotes the square diagonal matrix with the elements of the given vector on the diagonal. Moreover

$$\boldsymbol{\Lambda}^{\mathrm{T}} = [\hat{\lambda}_1, \hat{\lambda}_2, \ldots, \hat{\lambda}_L] \tag{15}$$

is the vector of estimated non-centrality parameters. Note that $\hat{\lambda}_j$ corresponds to the estimated non-centrality parameter for the distribution of $\mathcal{T}_j$ under $\mathcal{H}_1$ [as defined in (12)]. Results of (13) are used in subsequent sections in order to derive an optimal weight vector.

4.1 Deflection-maximising fusion rule

In this section, we seek to maximise deflection criterion over the class of soft decision-based cooperative CS detectors of the form (9). This performance measure is particularly appropriate for weak signal detection [21]. After some manipulation (omitted), we can obtain the deflection of cooperative detector as

$$D(\boldsymbol{w}) \triangleq \frac{(E[\mathcal{T}_{\mathrm{C}}|\mathcal{H}_1] - E[\mathcal{T}_{\mathrm{C}}|\mathcal{H}_0])^2}{\mathrm{Var}[\mathcal{T}_{\mathrm{C}}|\mathcal{H}_0]} = \frac{1}{4N}\frac{(\boldsymbol{\Lambda}^{\mathrm{T}}\boldsymbol{w})^2}{\boldsymbol{w}^{\mathrm{T}}\boldsymbol{w}} \tag{16}$$

We define the deflection-maximising distributed detector as the one that maximises the above expression. This method actually maximises the normalised difference between the conditional means of the test statistic at FC, so it should lead to a high probability of detection. Recently, another measure for evaluating the detection performance, called the MDC, [19] has been introduced. This criterion is defined similar to (16), except that in the denominator $\mathrm{Var}[\mathcal{T}_{\mathrm{C}}|\mathcal{H}_0]$ is replaced by $\mathrm{Var}[\mathcal{T}_{\mathrm{C}}|\mathcal{H}_1]$. In the following, we propose a new generalised metric that comprises both the CDC and the MDC ($p \in \{0, 1\}$)

$$D_{\mathrm{g}}(\boldsymbol{w}) \triangleq \frac{(E[\mathcal{T}_{\mathrm{C}}|\mathcal{H}_1] - E[\mathcal{T}_{\mathrm{C}}|\mathcal{H}_0])^2}{p\ \mathrm{Var}[\mathcal{T}_{\mathrm{C}}|\mathcal{H}_0] + (1-p)\mathrm{Var}[\mathcal{T}_{\mathrm{C}}|\mathcal{H}_1]} \tag{17}$$

which could be simplified to the conventional DC for $p = 1$ and the modified DC for $p = 0$. Thus, we can derive

$$D_{\mathrm{g}}(\boldsymbol{w}) = \frac{1}{4}\frac{(\boldsymbol{\Lambda}^{\mathrm{T}}\boldsymbol{w})^2}{\boldsymbol{w}^{\mathrm{T}}\boldsymbol{\Upsilon}\boldsymbol{w}} \tag{18}$$

with

$$\boldsymbol{\Upsilon} = N\boldsymbol{I}_L + (1-p)\mathbf{diag}(\boldsymbol{\Lambda}), \quad p = 0, 1 \tag{19}$$

According to (18), we introduce the deflection-maximising weight coefficients as

$$\boldsymbol{w}_{\mathrm{g}}^{\mathrm{opt}} = \arg \max_{\boldsymbol{w}\geq\mathbf{0}, ||\boldsymbol{w}||_2=1} \left\{\frac{(\boldsymbol{\Lambda}^{\mathrm{T}}\boldsymbol{w})^2}{\boldsymbol{w}^{\mathrm{T}}\boldsymbol{\Upsilon}\boldsymbol{w}}\right\} \tag{20}$$

whose optimal weight vector is denoted by $\boldsymbol{w}_{\mathrm{g}}^{\mathrm{opt}}$. Here, $\|\cdot\|_2$ denotes the Euclidian norm. In order to achieve a unique solution for the optimisation problem at hand, we confine the weight vector to have unit norm.

The problem (20) can be transformed into the problem of global maximisation of the Rayleigh quotient [22] of the vector $\boldsymbol{w}$. If $\boldsymbol{\Upsilon} = \boldsymbol{\Upsilon}^{1/2}\boldsymbol{\Upsilon}^{\mathrm{T}/2}$ be the Cholesky decomposition of $\boldsymbol{\Upsilon}$, then replacing $\boldsymbol{w} = \boldsymbol{\Upsilon}^{-1/2}\mathbf{v}$ leads to

$$\frac{(\boldsymbol{\Lambda}^{\mathrm{T}}\boldsymbol{w})^2}{\boldsymbol{w}^{\mathrm{T}}\boldsymbol{\Upsilon}\boldsymbol{w}} = \frac{\boldsymbol{v}^{\mathrm{T}}\boldsymbol{\Upsilon}^{-\mathrm{T}/2}\boldsymbol{\Lambda}\boldsymbol{\Lambda}^{\mathrm{T}}\boldsymbol{\Upsilon}^{-1/2}\boldsymbol{v}}{\boldsymbol{v}^{\mathrm{T}}\boldsymbol{v}} \triangleq \frac{\boldsymbol{v}^{\mathrm{T}}\boldsymbol{c}\boldsymbol{v}}{\boldsymbol{v}^{\mathrm{T}}\boldsymbol{v}} \tag{21}$$

where $\boldsymbol{c} \triangleq \boldsymbol{\Upsilon}^{-\mathrm{T}/2}\boldsymbol{\Lambda}\boldsymbol{\Lambda}^{\mathrm{T}}\boldsymbol{\Upsilon}^{-1/2}$. Based on the global maximisation theorem on Rayleigh quotients [22], the maximum of right-hand side of (21) is the maximum eigenvalue of the matrix $\boldsymbol{c}$. Furthermore, the vector $\boldsymbol{v}$ that maximises the quotient is the eigenvector corresponding to the maximum eigenvalue.

Consequently, the eigenvector corresponding to the maximum eigenvalue of the positive semidefinite matrix $\boldsymbol{c}$ is $\boldsymbol{v}_{\mathrm{opt}} = \boldsymbol{\Upsilon}^{-\mathrm{T}/2}\boldsymbol{\Lambda}$. Normalising the results gives the optimal weight vector

$$\boldsymbol{w}_{\mathrm{g}}^{\mathrm{opt}} = \frac{\boldsymbol{\Upsilon}^{-1/2}\boldsymbol{\Upsilon}^{-\mathrm{T}/2}\boldsymbol{\Lambda}}{||\boldsymbol{\Upsilon}^{-1/2}\boldsymbol{\Upsilon}^{-\mathrm{T}/2}\boldsymbol{\Lambda}||_2} \tag{22}$$

Finally, the deflection-maximising linear fusion rule can be expressed as

$$S_{\mathrm{g}}^{\mathrm{opt}}(\boldsymbol{\Gamma}) = \frac{1}{||\boldsymbol{\Upsilon}^{-1/2}\boldsymbol{\Upsilon}^{-\mathrm{T}/2}\boldsymbol{\Lambda}||_2}\boldsymbol{\Lambda}^{\mathrm{T}}\boldsymbol{\Upsilon}^{-1/2}\boldsymbol{\Upsilon}^{-\mathrm{T}/2}\boldsymbol{\Gamma} \tag{23}$$

Performance evaluations for the above method is provided in Section 6.

4.2 Sum detector fusion rule

A straightforward detector that we can obtain from (9) is the sum detector. If we set all the weights w_i identical ($i = 1, 2, \ldots, L$), with the constraint $\|\boldsymbol{w}\|_2 = 1$, we obtain $w_i = 1/\sqrt{L}$. Therefore

$$\mathcal{T}_{\mathrm{s.d.}} = \frac{1}{\sqrt{L}}\sum_{j=1}^{L}\mathcal{T}_j \tag{24}$$

This is the cooperative sum-detector proposed in [11]. We note that (24) is in fact a scaled log-likelihood ratio fusion rule. As we will show in Section 6, this test does not leads to a high probability of detection, as compared with proposed deflection-maximising fusion rules. This is because of the fact that the thresholds of hypothesis tests at local SUs as well as FC are not obtained through system-wide optimisation.

Some straightforward calculations yield the following threshold

$$\eta = \frac{1}{\sqrt{L}}\mathcal{Q}_{\chi^2_{2NL}}^{-1}(P_{\mathrm{f}}) \tag{25}$$

and detection probability

$$P_{\mathrm{d}} = \mathcal{Q}_{\chi^2_{2NL}(\Sigma\lambda_i)}(\mathcal{Q}_{\chi^2_{2NL}}^{-1}(P_{\mathrm{f}})) \tag{26}$$

for the cooperative sum detector.

doi: 10.1049/iet-com.2011.0269

5 Proposed cooperative hypothesis testing

5.1 Threshold setting at FC

In order to perform statistical test and analytically characterise the proposed methods, we should calculate the distribution of the test statistics under both hypotheses. However an efficient exact distribution of the weighted sum of independent chi-square random variables has not been derived yet. Therefore we derive an approximate distribution for the linear combination of chi-square variables, which is a common technique in statistics [23], as well as wireless communications [24]. This approximation, which enables the resultant detection performance to be analytically characterised, will be confirmed subsequently by numerical results.

First, we investigate the distribution of $\mathcal{T}_{\mathrm{C}}$ under null hypothesis. If we assume that $\mathcal{T}_j \sim \chi^2_{2N}$ be independent central chi-square variables under null hypothesis, we can approximately write

$$\mathcal{T}_{\mathrm{C}|\mathcal{H}_0} = \sum_{j=1}^{\mathrm{L}} w_j \mathcal{T}_j \overset{\mathrm{a}}{\sim} \alpha_0 \chi^2_{\beta_0} \tag{27}$$

where $\overset{\mathrm{a}}{\sim}$ means 'is approximately distributed as'. We refer to this technique as two-moment fitting method. By equating the mean and variances (i.e. first- and second-order cumulants) of the left- and right-hand side of (27), the coefficients can be calculated as

$$\alpha_0 = \frac{\sum_{j=1}^{L} w_j^2}{\sum_{j=1}^{L} w_j}, \quad \beta_0 = \frac{2N(\sum_{j=1}^{L} w_j)^2}{\sum_{j=1}^{L} w_j^2} \tag{28}$$

Thus, the threshold at the FC can be calculated as

$$\eta \simeq \alpha_0 \mathcal{Q}^{-1}_{\chi^2_{\beta_0}}(P_{\mathrm{f}}) = \alpha_0 \mathcal{F}^{-1}_{\chi^2_{\beta_0}}(1 - P_{\mathrm{f}}) \tag{29}$$

where $\mathcal{F}^{-1}_{\chi^2_r}(x)$ is the inverse cumulative distribution of central chi-square random variable.

5.2 Analytical performance analysis

For analytical performance evaluation of proposed scheme, we need the asymptotic distribution of $\mathcal{T}$ under alternative hypothesis (denoted by $\mathcal{T}_{C|\mathcal{H}_1}$). We keep in mind that the test statistics of different SUs are asymptotically independent. Hence, if we assume $\mathcal{T}_j \sim \chi'^2_{2N}(\hat{\lambda}_j)$, using the same procedure as (27) and (28), we can calculate the coefficients under $\mathcal{H}_1$

$$\alpha_1 = \frac{2\sum_{j=1}^{L} w_j^2(N + \hat{\lambda}_j)}{\sum_{j=1}^{L} w_j(2N + \hat{\lambda}_j)}, \quad \beta_1 = \frac{(\sum_{j=1}^{L} w_j(2N + \hat{\lambda}_j))^2}{2\sum_{j=1}^{L} w_j^2(N + \hat{\lambda}_j)} \tag{30}$$

Computation of above parameters requires the knowledge of non-centrality parameters $\{\hat{\lambda}_j\}_{j=1}^{L}$. This is a reasonable assumption as this information is estimated in local sensing step.

Fig. 1 provides a basis to judge the adequacy of two-moment fitting method for $\mathcal{T}_{\mathrm{C}|\mathcal{H}_0}$ and $\mathcal{T}_{\mathrm{C}|\mathcal{H}_1}$. The two-moment distribution fit gives an expedient and efficient procedure for the weighted sum under null hypothesis. In other words, evaluation of the threshold from null hypothesis distribution is almost accurate. However, under $\mathcal{H}_1$ it has not sufficient accuracy. Therefore by employing the more-accurate three-moment approximation for weighted sum of non-central chi-square distributions [23],

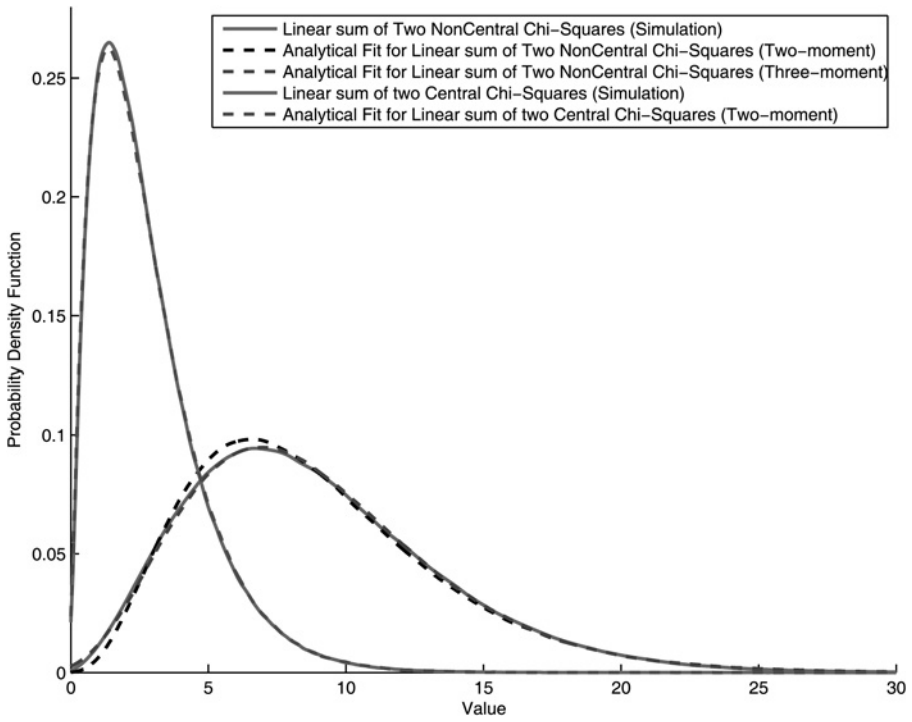

Fig. 1 *Comparison of analytical and simulated PDFs of sum of two chi-square distributions under $\mathcal{H}_0$ and $\mathcal{H}_1$ (weighted sums are $0.578\chi^2_2 + 0.815\chi^2_2$ and $0.578\chi_2'^2(5.272) + 0.815\chi_2'^2(3.753)$)*

we rise the accuracy for analytical performance evaluation case.

Based on the above discussion, we propose the following approximation for distribution of linear fusion rule under alternative hypothesis

$$\mathcal{T}_{\mathrm{C}|\mathcal{H}_1} \overset{\mathrm{a}}{\sim} \rho\chi_r^2 + d \tag{31}$$

It can be shown that the first three cumulants of both sides of (31) are

$$\begin{aligned}
\kappa_1 &= \sum_{i=1}^{L} w_i(2N + \hat{\lambda}_i) = \rho r + d \\
\kappa_2 &= \sum_{i=1}^{L} 2w_i^2(2N + 2\hat{\lambda}_i) = 2\rho^2 r \\
\kappa_3 &= \sum_{i=1}^{L} 8w_i^3(2N + 3\hat{\lambda}_i) = 8\rho^3 r
\end{aligned} \tag{32}$$

where κ_i is the cumulant of order i. Solving the above system of equations for ρ, r and d yields $r = c_2^3/c_3^2$, $\rho = c_3/c_2$ and $d = c_1 - c_2^2/c_3$, where $c_j \triangleq \sum_{i=1}^{L} w_i^j(2N + j\hat{\lambda}_i)$, $j = 1, 2, 3$.

Therefore we attain the following detection performance for the proposed cooperative sensing scheme

$$\begin{aligned}
P_{\mathrm{d}} &\simeq Q_{\chi_r^2}\left(\frac{\alpha_0 Q^{-1}_{\chi^2_{\beta_0}}(P_{\mathrm{f}}) - d}{\rho}\right) \\
&= \frac{\Gamma((r/2), (\{\alpha_0 Q^{-1}_{\chi^2_{\beta_0}}(P_{\mathrm{f}}) - d\})/2\rho)}{\Gamma(r/2)}
\end{aligned} \tag{33}$$

As we will show in Section 6, this analytical performance evaluation matches well with the Monte-Carlo performance estimation results.

6 Discussions and simulation results

The primary network is an IEEE 802.11a wireless local area network (WLAN) with orthogonal frequency-division multiplexing (OFDM) transmissions. Complex symbols, which are inputs to the inverse fast Fourier transform (IFFT) at the PU transmitter, are chosen from a quadrature phase-shift keying (QPSK) constellation. Following the settings in IEEE 802.11a protocol, we set the values of fast Fourier transform (FFT) length, number of occupied channels, length of guard interval, symbol rate and sampling rate as $N_{\mathrm{fft}} = 64$, $N_{\mathrm{occ}} = 52$, $N_{\mathrm{g}} = 16$, $R_{\mathrm{sym}} = 250$ Ksym/s, $R_{\mathrm{s}} = 20$ MHz, respectively. For all simulations, discrete-time baseband processing is assumed. Except otherwise stated, each SU uses the cycle frequency $\alpha = 1/(N_{\mathrm{fft}} + N_{\mathrm{g}})$ and the time-lag parameter $\tau = N_{\mathrm{fft}}$. For cooperative scenarios, it is assumed that ten SUs exist in network (i.e. $L = 10$).

In all simulations with fixed signal length, the detection time at each SU is assumed to be 50 OFDM blocks. Therefore the number of samples for the CAF estimate at the SU is $50N_{\mathrm{u}}$. This approximately corresponds to the sensing time of 0.2 ms for an OFDM system having bandwidth of 20 MHz. The length of Kaiser window and its β parameter in CS detectors are chosen to be 2048 and $\beta = 10$, respectively. See Appendix 1 for details. The desired probability of false alarm is set at 0.01. The average channel SNR in ith observation channel is defined as $\mathrm{SNR}_i = 10\log_{10}(\sigma_x^2/N_i)$, where σ_x^2 and N_i are the variances of PU's signal and noise, respectively.

The simulations are performed over a sensing duration of $x(n = 1{:}\ M)$. In this interval, each SU independently performs local spectrum sensing, computes its test statistic and estimates the non-centrality parameter. Furthermore, in each sensing slot, the PU is either active or inactive. After computing the test statistic, each SU sends its decision statistic (which is also the value of the locally estimated non-centrality parameter) to the FC. Based on received decision statistics, the deflection-optimal optimal weights are computed. In the next sensing slot, the above-mentioned states should be repeated, so the weight coefficients are updated in each sensing duration. Except otherwise stated, each simulation curve is obtained over 50 000 independent Monte-Carlo realisations.

6.1 Performance of local sensing

Fig. 2 compares the agreement between analytical and simulated detection probability for local sensing case. The analytical curves are obtained using (6) and (7). Since, in practice, the true value of λ is not available at the SU, we use the estimated value $\hat{\lambda}$ in (7). In fact, as the signal length grows, the agreement between theoretical and simulation receiver operating characteristics (ROC) curves improves. Results show that the asymptotic equations in (5) hold true even in relatively low sensing times (i.e. non-asymptotic cases). Also we can see that as the sensing time increases, the detection performance improves. Since sensing time in secondary networks is limited, one can resort to cooperative sensing. This leads to a reduction in sensing time while meeting a high probability of correct detection.

6.1.1 Impact of CR velocity: In order to inspect the cyclostationarity of the received faded signal, we characterise the impact of Rayleigh fading impairments on the received CAF. In fact, the received CAF is directly proportional to the autocorrelation of the channel fading process (for detailed proof see Appendix 2) (Fig. 3)

$$R^{\alpha}_{yy^*}(\tau) = R_h(\tau)R^{\alpha}_{xx^*}(\tau) \tag{34}$$

If we assume the fading process to be wide-sense stationary, its autocorrelation function can be formulated using the well-known Jake's model as $R_h(k) = E[h(n)h^*(n + k)] = J_0(k\omega_{\mathrm{d}})$, where J_0 is the zero-order Bessel function of the first kind [20]. In this expression we assume that the mean-square transfer through the channel is normalised to unity, and $\omega_{\mathrm{d}} = 2\pi f_{\mathrm{d}}$ is the maximum angular Doppler frequency, in which $f_{\mathrm{d}} \triangleq f_{\mathrm{c}}\upsilon/c$, c is the speed of light, f_{c} is the carrier frequency and υ is the mobile velocity. Despite the problems associated with this model, it is adequate to explain many of the commonly encountered fading problems in practice [10]. Adopting this model, we can derive

$$R^{\alpha}_{yy^*}(\tau) = J_0(\omega_{\mathrm{d}}\tau)R^{\alpha}_{xx^*}(\tau) \tag{35}$$

This demonstrates that the detection loss caused by fading depends on maximum Doppler shift as well as time lag used by the CS detector. Since the time lag is directly related to the PU signal type, impact of fading on the

doi: 10.1049/iet-com.2011.0269

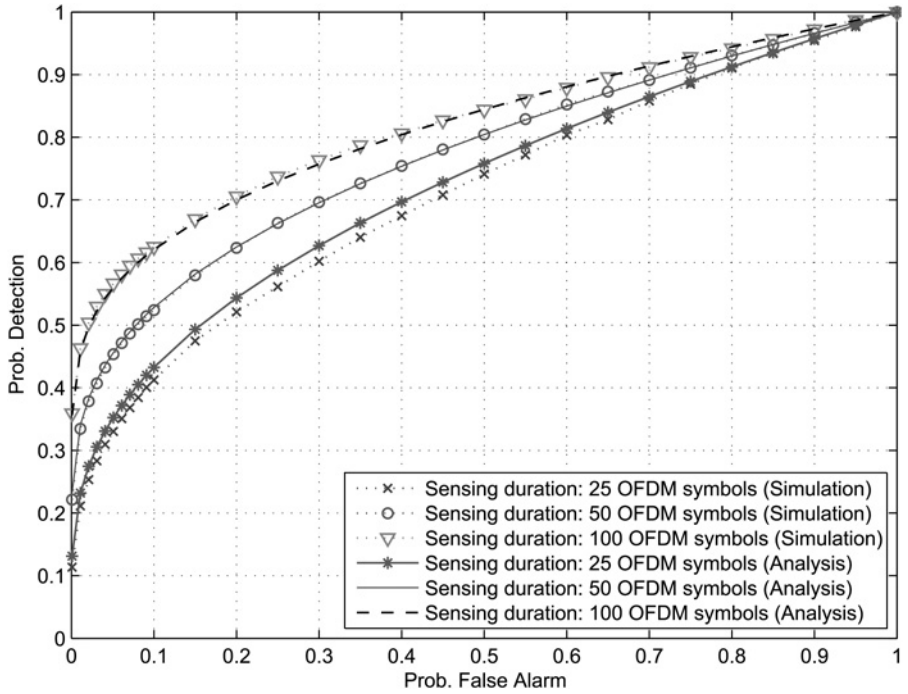

Fig. 2 *Analytical against simulated performances of local sensing for different signal lengths over frequency-flat Rayleigh fading channel with SNR = −8 dB*

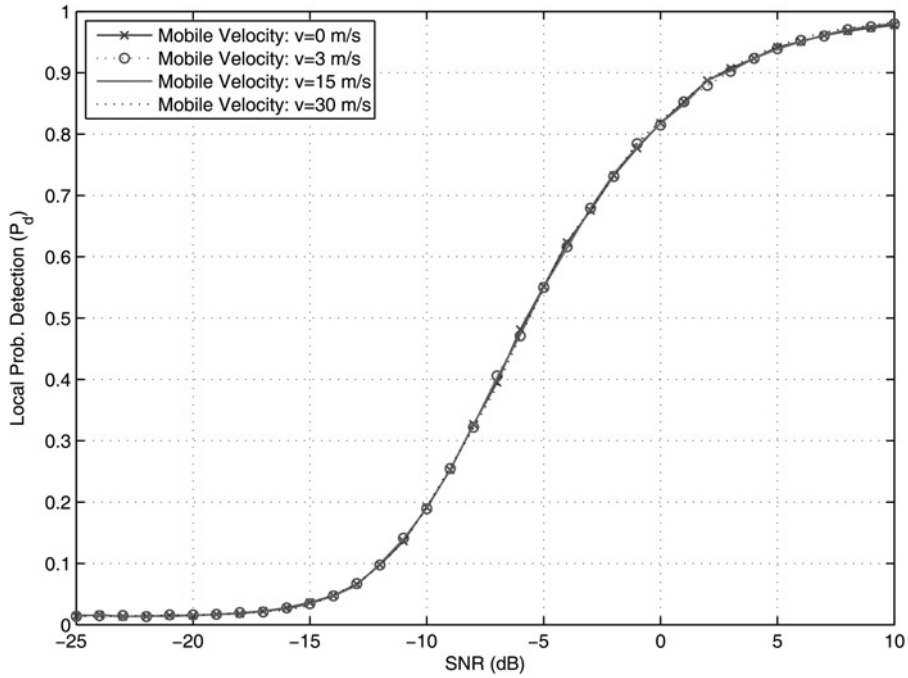

Fig. 3 *Local detection performance of cyclostationarity-based sensing for different mobile velocities in Rayleigh fading channels*

cyclostationarity of received signal is dependent on primary signal type.

For example, if the primary signal is a WLAN IEEE 802.11a signal, the time lag in CS detectors must be set to $\tau \simeq 3.2$ μs. For practical applications and carrier frequency equal to 5 GHz, if we assume that $\Delta f_d \leq 1$ kHz, deviation of $\omega_d \tau$ is less than 0.02. Hence, the amount of cyclostationarity degradation because of an increase in mobile velocity of CR should be negligible. We confirm this proposition by simulation of CS detector with above-mentioned primary signal. As it is evident, from Fig. 3, local probability of detection remains unchanged for different mobile velocities. Therefore the proposed spectrum sensing technique has relatively an acceptable performance in high mobile speeds.

6.2 Performance of cooperative sensing

In this section, we will compare the proposed cyclostationarity-based linear fusion rules. We firstly examine the validity of the proposed approximation for the distribution of the linear fusion rule under $\mathcal{H}_0$. Since the threshold of the proposed linear fusion rule is identified by

the cumulative distribution function (CDF) of test statistic under $\mathcal{H}_0$, we will evaluate the CDF of proposed test statistic. To this end, we generate the white Gaussian noise over 100 000 independent realisations. The block length of the noise signal is $M = 4000$ samples. As we can see from Fig. 4, the proposed method well approximates the simulated CDF of the test statistic $\mathcal{T}_C$ under null hypothesis, so the threshold at the FC can be accurately obtained by employing the proposed low-complexity approximation technique.

Analytical and simulated ROC curves for proposed cyclostationarity-based linear fusion rule are shown in Fig. 5 under different average SNRs. Simulation results confirm the proposed analytical approximation derived in (33). Conventional deflection-maximising method is used for calculating the weight vector. Simulations are performed in Rayleigh fading environments with the assumption that ten SUs exist in network. Different CRs have different average channel SNRs for their observation channels. We assume that $\boldsymbol{\gamma} = [\bar{\gamma} - 16, \bar{\gamma} - 12, \bar{\gamma} - 8,$

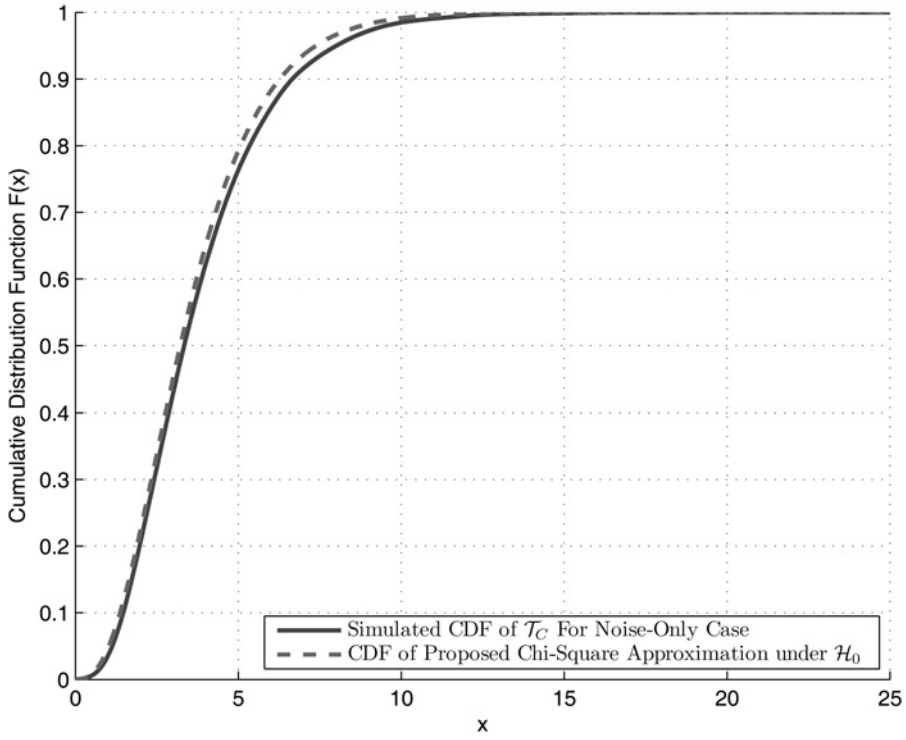

Fig. 4 *Validity of the proposed low-complexity approximate distribution for the test statistic at the FC under $\mathcal{H}_0$ ($p = 0$)*

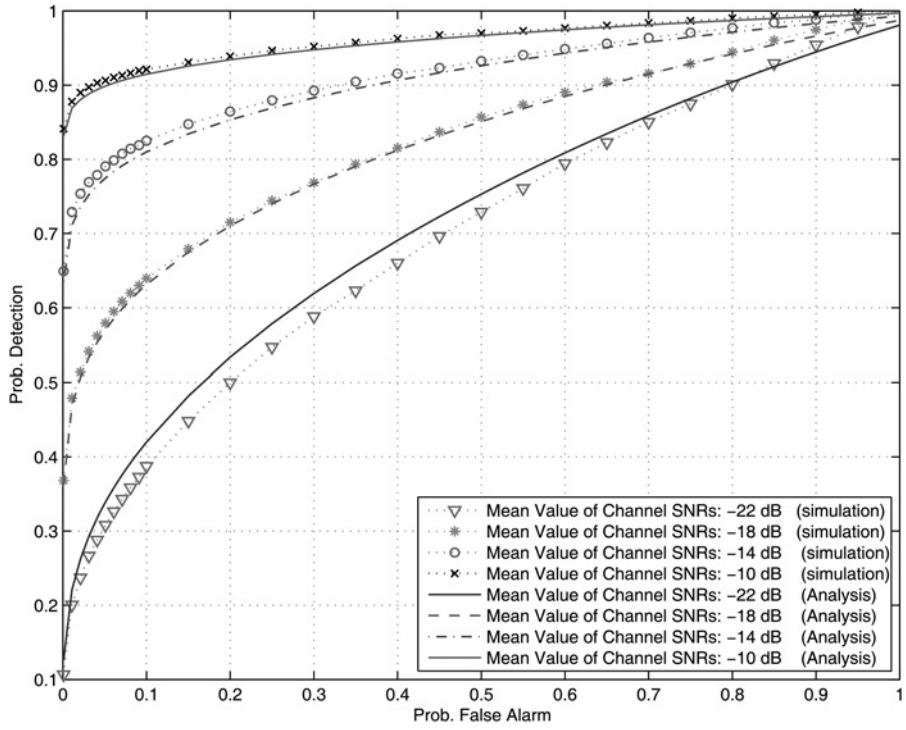

Fig. 5 *Analytical against simulated ROC curves for proposed linear fusion rule over frequency-flat Rayleigh fading channels ($p = 1$)*

doi: 10.1049/iet-com.2011.0269

$\bar{\gamma}-4, \bar{\gamma}, \bar{\gamma}, \bar{\gamma}+4, \bar{\gamma}+8, \bar{\gamma}+12, \bar{\gamma}+16]$, where $\boldsymbol{\gamma} = [\mathrm{SNR}_1, \ldots, \mathrm{SNR}_L]$ is the vector of average channel SNRs and $\bar{\gamma}$ is the arithmetic mean value of all the channel SNRs in decibels. The analytical curves are obtained from (33).

Next, we would like to evaluate the performance of different CS-based cooperative sensing methods over fading channels. Fig. 6 depicts the ROC performance curves for proposed methods in frequency-flat Rayleigh fading environment. It is evident that the conventional deflection coefficient maximisation (CDFM) method outperforms the other ones in fading environment. Different secondary users experience independent fading with different channel SNR. Note that there is 35 dB difference between the largest and the smallest channel SNRs, so that there is a significant variation in the observed channel SNRs.

Fig. 7 shows the probability of missed detection as a function of mean value of channel SNRs in frequency-flat Rayleigh fading environment. It is evident that the CDFM method has the lowest probability of missed detection in both low and high SNR conditions. This confirms the superiority of CDFM method, independent of channel SNRs. The vector of channel SNRs ($\boldsymbol{\gamma}$) is defined as in Fig. 5.

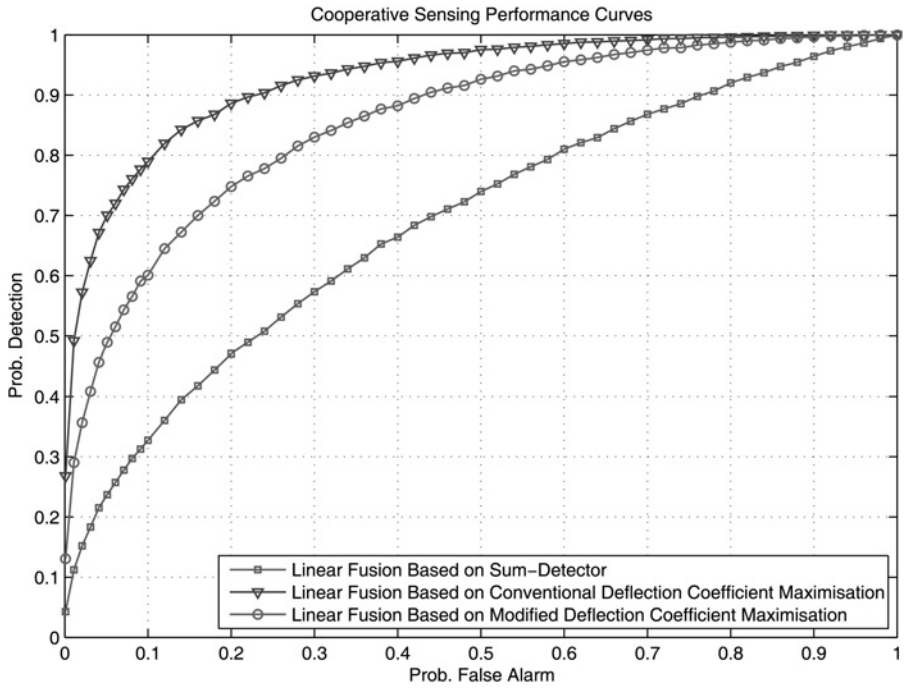

Fig. 6 *ROC curves for various cyclostationarity-based cooperative sensing methods over frequency-flat Rayleigh fading channel* $\boldsymbol{\gamma} = [-45.8, -33.5, -30.7, -35.1, -26.6, -21.2, -19.3, -15.8, -15.1, -10.2]$ *(in dB)*

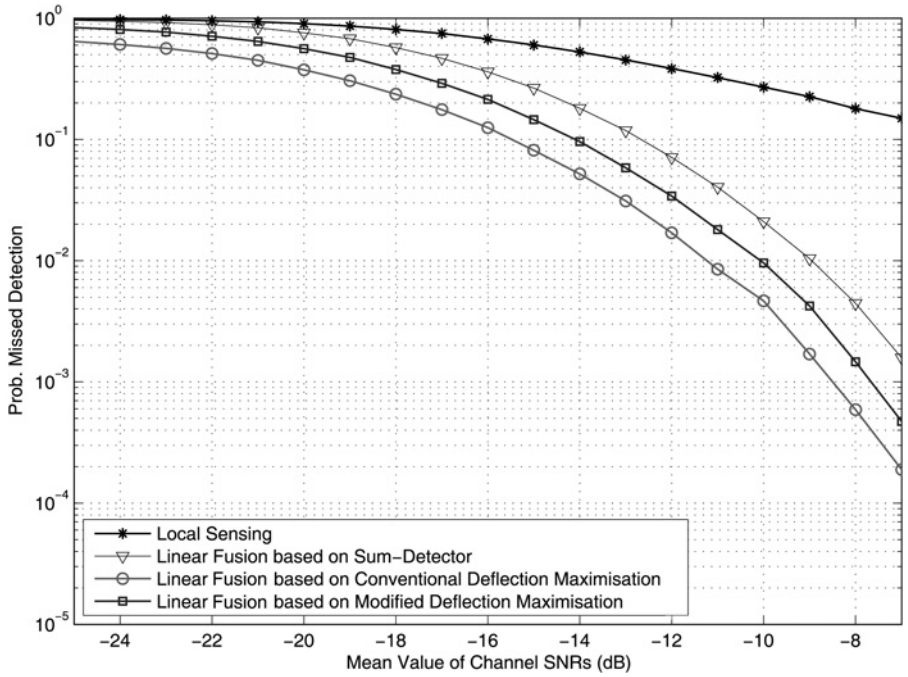

Fig. 7 *Probability of missed detection against the mean value of channel SNRs* ($\bar{\gamma}$) *in frequency-flat Rayleigh fading channels*

7 Conclusions

In this paper, we have developed soft CS -based CSS method based on DC maximisation at the FC. Furthermore, we have derived low-complexity and efficient closed-form approximations to the distribution of the proposed linear fusion rule under both null and alternative hypotheses. These approximations enable performing threshold setting at the FC and facilitates the performance analysis and comparison. Simulation results have demonstrated that the proposed deflection-maximising scheme exhibits comparable performance with the sum-detector scheme. In addition, simulation results confirm the proposed analytical performance evaluation. We have further studied the impact of secondary user's mobility on the local sensing performance through analysis as well as simulation.

8 Acknowledgment

This work was supported in part by the Research Institute for ICT (ITRC) under project number of T-8755-500.

9 References

1 Mitola, J.: 'Cognitive radio: an integrated agent architecture for software defined radio'. PhD dissertation, KTH Royal Institute of Technology, Sweden, May 2000
2 Cabric, D., Mishra, S.M., Brodersen, R.W.: 'Implementation issues in spectrum sensing for cognitive radios'. Proc. 38th Asilomar Conf. Signals, Systems and Computers, 2004, vol. 1, pp. 772–776
3 Sridhara, K., Chandra, A., Tripathi, P.S.M.: 'Spectrum challenges and solutions by cognitive radio: an overview', *Wirel. Pers. Commun.*, 2008, **45**, (3), pp. 281–291
4 El-Hajj, W., Safa, H., Guizani, M.: 'Survey of security issues in cognitive radio networks', *J. Internet Technol.*, 2011, **12**, (2), pp. 181–198
5 Chen, Y., Cho, C., You, I., Chao, H.: 'A cross-layer protocol of spectrum mobility and handover in cognitive lte networks', *Simul. Model. Pract. Theory*, 2011, **19**, (8), pp. 1723–1744
6 Arslan, H.: 'Cognitive radio, software defined radio, and adaptive wireless systems' (Springer, 2007)
7 Huang, L., Gao, Z., Guo, D., Chao, H., Park, J.: 'A sensing policy based on the statistical property of licensed channel in cognitive network', *Int. J. Internet Protocol Technol.*, 2010, **5**, (4), pp. 219–229
8 Gao, Z., Huang, L., Yao, Y., Wu, T.: 'Performance analysis of a busy cognitive multi-channel mac protocol', *J. Internet Technol.*, 2011, **11**, (3), pp. 299–306
9 Tandra, R., Sahai, A.: 'Fundamental limits on detection in low SNR under noise uncertainty'. Proc. Int. Conf. Wireless Networks, Communication and Mobile Computing, Maui, HI, June 2005, vol. 1, pp. 464–469
10 Haykin, S., Thomson, D.J., Reed, J.H.: 'Spectrum sensing for cognitive radio', *Proc. IEEE*, 2009, **97**, (5), pp. 849–877
11 Lunden, J., Koivunen, V., Huttunen, A., Poor, H.V.: 'Collaborative cyclostationary spectrum sensing for cognitive radio systems', *IEEE Trans. Signal Process.*, 2009, **57**, (11), pp. 4182–4195
12 Oner, M., Jondral, F.: 'Air interface identification for software radio systems', *Int. J. Electron. Commun. (AEU)*, 2007, **61**, (2), pp. 104–117
13 Ma, J., Li, G.Y., Juang, B.H.: 'Signal processing in cognitive radio', *Proc. IEEE*, 2009, **97**, (5), pp. 805–823
14 Sadeghi, H., Azmi, P.: 'Cyclostationarity-based cooperative sensing for cognitive radio networks'. Proc. Int. Symp. Telecommunication (IST 2008), August 2008, pp. 429–434
15 Dandawaté, A.V., Giannakis, G.B.: 'Statistical tests for presence of cyclostationarity', *IEEE Trans. Signal Process.*, 1994, **42**, (9), pp. 2355–2369
16 Mosquera, C., Scalise, S., Lopez-Valcarce, R.: 'Non-data-aided symbol rate estimation of linearly modulated signals', *IEEE Trans. Signal Process.*, 2008, **56**, (2), pp. 664–675
17 Mazet, L., Loubaton, P.H.: 'Cyclic correlation based symbol rate estimation'. 33rd Asilomar Conf. Signals, Systems and Computers, Pacific Grove, CA, 1999, vol. 1, pp. 1008–1012
18 Varshney, P.K.: 'Distributed detection and data fusion' (Springer-Verlag, New York, 1997)
19 Quan, Z., Cui, S., Sayed, A.H.: 'Optimal linear cooperation for spectrum sensing in cognitive radio networks', *IEEE J. Sel. Topics Signal Process.*, 2008, **2**, (1), pp. 28–40
20 Proakis, J.G., Salehi, M.: 'Digital communications' (McGraw-Hill, New York, 2008, 5th edn.)
21 Kay, S.M.: 'Fundamentals of statistical signal processing, vol. II: detection theory' (Prentice Hall, 1998)
22 Schott, J.R.: 'Matrix analysis for statistics' (Wiley-Interscience, 1997)
23 Imhof, J.P.: 'Computing the distribution of quadratic forms in normal variables', *Biometrika*, 1961, **48**, (3), pp. 419–426
24 Zhang, Q.T., Liu, D.P.: 'A simple capacity formula for correlated diversity Rician fading channels', *IEEE Commun. Lett.*, 2002, **6**, (11), pp. 481–483

10 Appendix 1: Computation of covariance matrix

In each sensing slot, the $2N \times 2N$ dimensional covariance matrix $\boldsymbol{\Sigma}_{xx^*}$ can be estimated based on the received signal as follows [15]

$$\hat{\boldsymbol{\Sigma}}_{xx^*} = \begin{bmatrix} \mathrm{Re}\left\{\dfrac{\hat{\boldsymbol{Q}} + \hat{\boldsymbol{Q}}^{(*)}}{2}\right\} & \mathrm{Im}\left\{\dfrac{\hat{\boldsymbol{Q}} - \hat{\boldsymbol{Q}}^{(*)}}{2}\right\} \\ \mathrm{Im}\left\{\dfrac{\hat{\boldsymbol{Q}} + \hat{\boldsymbol{Q}}^{(*)}}{2}\right\} & \mathrm{Re}\left\{\dfrac{\hat{\boldsymbol{Q}}^{(*)} - \hat{\boldsymbol{Q}}}{2}\right\} \end{bmatrix} \tag{36}$$

where the (m, n)th entries of the two covariance matrices $\hat{\boldsymbol{Q}}$ and $\hat{\boldsymbol{Q}}^{(*)}$ are given by $(1 \le m, n \le N)$

$$\hat{\boldsymbol{Q}}_{mn} = \frac{1}{MP} \sum_{s=-((P-1)/2)}^{(P-1)/2} W_P(s) F_{\tau_n}\left(\vartheta - \frac{s}{M}\right) F_{\tau_m}\left(\vartheta + \frac{s}{M}\right) \tag{37}$$

$$\hat{\boldsymbol{Q}}^{(*)}_{mn} = \frac{1}{MP} \sum_{s=-((P-1)/2)}^{(P-1)/2} W_P(s) F^*_{\tau_n}\left(\vartheta + \frac{s}{M}\right) F_{\tau_m}\left(\vartheta + \frac{s}{M}\right) \tag{38}$$

Here, W_P is a normalised smoothing window with an odd length P, and $F_\tau(\vartheta) = \sum_{t=1}^{M} x(t)x^*(t+\tau)\mathrm{e}^{-\mathrm{j}2\pi\vartheta t}$.

11 Appendix 2: Impact of Rayleigh fading

The CAF of the received signal $y(n)$ from the time-varying Rayleigh fading channel can be calculated as

$$\begin{aligned} R^{\alpha}_{yy^*}(\nu) &= \lim_{M\to\infty} \frac{1}{M} \sum_{n=1}^{M} \mathbb{E}\{[h(n)x(n) + w(n)] \\ &\quad \times [h^*(n)x^*(n+\nu) + w^*(n+\nu)]\} \times \mathrm{e}^{-\mathrm{j}2\pi\alpha n} \\ &= \lim_{M\to\infty} \frac{1}{M} \sum_{n=1}^{M} \mathbb{E}\{h(n)h^*(n+\nu)\} \\ &\quad \times \mathbb{E}\{[x(n)x^*(n+\nu)]\}\mathrm{e}^{-\mathrm{j}2\pi\alpha n} \\ &\quad + \lim_{M\to\infty} \frac{1}{M} \sum_{n=1}^{M} \mathbb{E}\{[w(n)w^*(n+\nu)]\}\mathrm{e}^{-\mathrm{j}2\pi\alpha n} \\ &= \mathbb{E}\{h(n)h^*(n+\nu)\} \times R^{\alpha}_{xx^*}(\nu) + R^{\alpha}_{ww^*}(\nu) \\ &= R_h(\nu) R^{\alpha}_{xx^*}(\nu) \end{aligned} \tag{39}$$

where $R_h(\nu)$ is the autocorrelation of the channel fading process.

doi: 10.1049/iet-com.2011.0269